Oncogene (2016) **35,** 558–566

www.nature.com/onc

OPEN

ORIGINAL ARTICLE

Development of secondary mutations in wild-type and mutant EZH2 alleles cooperates to confer resistance to EZH2 inhibitors

V Gibaja[1], F Shen[1], J Harari[1], J Korn[1], D Ruddy[1], V Saenz-Vash[1], H Zhai[1], T Rejtar[1], CG Paris[1], Z Yu[2], M Lira[1], D King[1], W Qi[2], N Keen[1], AQ Hassan[1] and HM Chan[1]

The histone methyltransferase Enhancer of Zeste Homolog 2 (EZH2) is frequently dysregulated in cancers, and gain-of-function (GOF) EZH2 mutations have been identified in non-Hodgkin lymphomas. Small-molecule inhibitors against EZH2 demonstrated anti-tumor activity in EZH2-mutated lymphomas and entered clinical trials. Here, we developed models of acquired resistance to EZH2 inhibitor EI1 with EZH2-mutated lymphoma cells. Resistance was generated by secondary mutations in both wild-type (WT) and GOF Y641N EZH2 alleles. These EZH2 mutants retained the substrate specificity of their predecessor complexes but became refractory to biochemical inhibition by EZH2 inhibitors. Resistant cells were able to maintain a high level of H3K27Me3 in the presence of inhibitors. Interestingly, mutation of EZH2 WT alone generated an intermediate resistance phenotype, which is consistent with a previously proposed model of cooperation between EZH2 WT and Y641N mutants to promote tumorigenesis. In addition, the findings presented here have implications for the clinical translation of EZH2 inhibitors and underscore the need to develop novel EZH2 inhibitors to target potential resistance emerging in clinical settings.

Oncogene (2016) **35,** 558–566; doi:10.1038/onc.2015.114; published online 20 April 2015

INTRODUCTION

Polycomb repressive complex 2 (PRC2) is required during normal embryonic development to maintain transcriptional repression of key developmental regulators.[1–3] Enhancer of Zeste Homolog 2 (EZH2) is the catalytic subunit of PRC2, which methylates H3K27 to repress transcription.[4] In cancers, EZH2 can be amplified and overexpressed, and elevated expression of EZH2 often correlates with poor prognosis.[5,6] Somatic activating mutations in the SET domain of EZH2 have been identified in several cancers, including follicular lymphoma and diffuse large B-cell lymphoma.[5,7,8] Tyr641 (Y641) is a hot-spot mutation in these lymphomas, and Y641 mutants have altered substrate specificity compared with WT EZH2. They show increased activity against di-methylated H3K27 and decreased activity toward unmethylated and monomethylated H3K27, resulting in a massive increase of the level of H3K27 trimethylation in the cell.[9,10] Increased EZH2 activity is believed to suppress cell cycle checkpoint genes and cellular differentiation programs to promote tumorigenesis.

We and others have reported the development of highly potent and selective small-molecule inhibitors against EZH2, including EI1, EPZ-6438 (also known as E7438), compound 3 and GSK126.[11–14] These inhibitors act competitively with respect to the methyl-group donor *S*-adenosyl methionine (SAM) to suppress the enzymatic activity of EZH2. They inhibit EZH2 WT and Y641 mutants and show high selectivity against other histone methyltransferases. In cells, EZH2 inhibitors specifically suppress H3K27 di- and trimethylation and reactivate the expression of target genes that had been repressed by PRC2 and H3K27 trimethylation, such as cell cycle checkpoint genes and GC-B-cell differentiation genes.[11,13–17] Potent anti-tumor activity has been observed in multiple cell lines and animal models, causing tumor regression in animal tumor models of diffuse large B-cell lymphoma,[11–15] malignant rhabdoid cancer[14,16] and ependymomas.[18] Two inhibitors (EPZ-6438 and GSK2816126) are now in clinical trials (http://clinicaltrials.gov/ct2/show/NCT01897571; http://clinicaltrials.gov/ct2/show/NCT02082977).

Acquired resistance is a major problem often limiting the long-term effectiveness of targeted cancer therapeutics. Resistance can be acquired through secondary mutations or amplification of the primary drug targets, or activation of bypass signaling pathways.[19] In this study, we investigated if cancer cells might also develop resistance to highly targeted epigenetic agents such as EZH2 inhibitors. A highly potent EZH2 inhibitor EI1[14] was used to generate resistance in a diffuse large B-cell lymphoma cell line KARPAS422, which contains a heterozygous EZH2 Y641N mutation (*EZH2*$^{wt/}$*EZH2*^{Y641N}). EI1 inhibits EZH2 WT and the Y641 mutant in biochemical assays with a half-maximal inhibition (IC_{50}) of 10–20 nM.[14] KARPAS422 is highly sensitive to EI1, which triggers growth arrest and apoptosis.[14] Acquired resistance was generated following prolonged exposure to EI1, and two novel missense mutations of EZH2 (Y111L and Y661D) were specifically identified in the resistant cells. Y661D occurred *cis* to the *EZH2*^{Y641N} allele, whereas Y111L occurred at the *EZH2*^{WT} allele. Biochemical characterization showed that these PRC2 mutant complexes retained the substrate specificity of the respective predecessor complexes. However, unlike PRC2^{WT} and PRC2^{Y641N} complexes, both PRC2^{Y111L} and PRC2$^{Y641N/Y661D}$ complexes were refractory to biochemical inhibition by EZH2 inhibitors. Furthermore, we showed that mutation of *EZH2*^{WT} allele alone (Y111L) was able to create a state of partial resistance. This is consistent with a

[1]Novartis Institutes for BioMedical Research, Cambridge, MA, USA and [2]China Novartis Institutes for BioMedical Research, Shanghai, China. Correspondence: Dr HM Chan or Dr AQ Hassan, Novartis Institutes for BioMedical Research, 250 Mass Avenue, Cambridge, MA 02139, USA.
E-mail: homan.chan@novartis.com or quamrul.hassan@novartis.com
Received 25 September 2014; revised 27 February 2015; accepted 6 March 2015; published online 20 April 2015

model in which $PRC2^{WT}$ cooperates with $PRC2^{Y641N}$ to elevate H3K27Me3 levels, thus promoting tumorigenesis. Therefore, targeting both EZH2 WT and Y641N should achieve most effective anti-tumor response.

In summary, this study has implications for clinical translation and further development of novel EZH2 inhibitors. First, monitoring EZH2 mutation status is warranted during clinical trials with patients with *de novo* and acquired resistance. Second, development of novel EZH2 inhibitors should be considered given the potential emergence of resistance in clinics.

RESULTS

Identification of resistance mutations in EZH2

EZH2 inhibitors have shown strong anti-proliferative responses in KARPAS422 lymphoma cells with complete tumor regression in xenograft models.[12,14,15] Here, we used the KARPAS422 cell line (K-P) as a model system to investigate potential resistance to EZH2 inhibitors. The experimental scheme is described in Figure 1a. K-P cells were cultured in the presence of 2 or 10 μM EI1 for 60 days. After 60 days of continuous treatment, we were able to derive resistant cells from the 2 μM treatment group (K-R2), whereas no resistant cells were recovered from the 10 μM treatment group. However, we were able to adapt K-R2 cells, in medium containing 10 μM EI1 for an additional 10 days, to obtain K-R10 cells. Fluorescence-activated cell sorting was performed to obtain 10 independent single-cell clones from each of the K-R2 and K-R10 pools, identified as K-R2#1-10 and K-R10#1-10, respectively (Figure 1a).

K-R2 and K-R10 cells were able to proliferate in medium with or without EI1, although they exhibit a slightly slower growth rate compared with K-P cells (Figure 1b). K-R2 and K-R10 cells were able to maintain H3K27Me3 levels in the presence of EI1 that were comparable to the basal levels of H3K27Me3 in K-P cells without

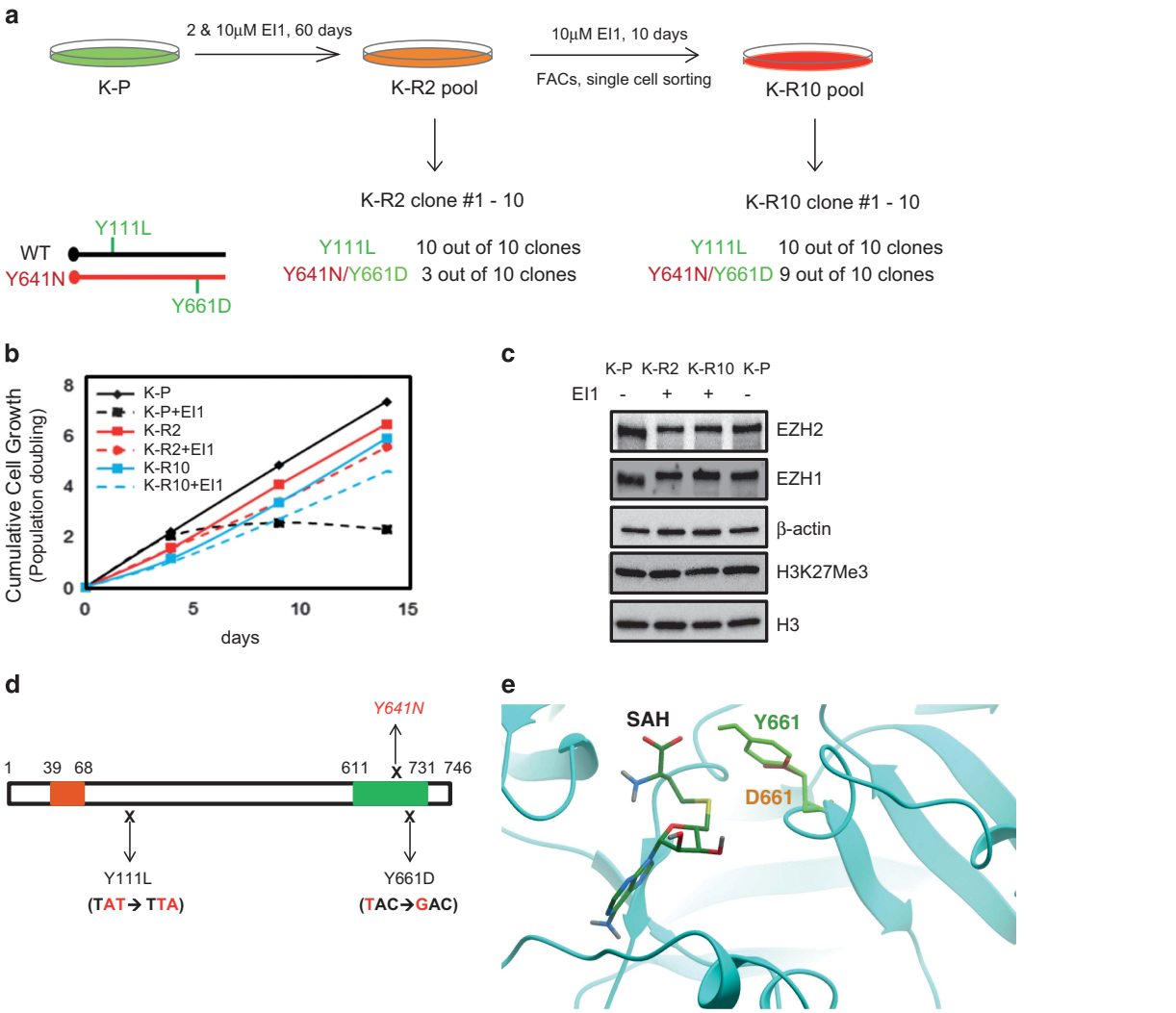

Figure 1. Identification of EZH2 resistance mutations in KARPAS422. (**a**) Schematic representation of the experimental procedure. K-P: KARPAS422-parental cells; K-R2 and K-R10: KARPAS422 cells resistant to 2 μM and 10 μM EI1, respectively. Y111L and Y661D mutations are indicated in different *EZH2* alleles. (**b**) Characterization of the growth kinetics of K-P, K-R2 and K-R10 cells. *Y*-axis indicates cumulative cell growth (population doubling). K-P and K-R10 cells were treated with 10 μM EI1 and K-R2 cells were treated with 2 μM EI1. (**c**) Western blots of EZH2, EZH1 and H3K27Me3 in the indicated samples. Histone H3 and β-actin were used as loading controls. K-R2 and K-R10 were cultured in 2 μM and 10 μM EI1, respectively. (**d**) Schematic representation of EZH2 domain structure. EZH2–EED interaction domain (red), and SET domain (green) are indicated. EZH2 Y641N mutation and codon changes associated with Y111L and Y661D mutation are indicated in red. (**e**) Structural model of Y661D in the EZH2 SET domain. A model of the EZH2 SET domain was derived from the homologous domain of GLP (EHMT1, PDB: 3HNA, resolution 1.5 Å). The backbone trace ribbon is blue, and the highlighted rendering of residue 661 is color-coded either green (wt-EZH2 Y661) or orange (mutant EZH2 D661). SAH is indicated in the image and visualization was generated using Molsoft ICM. FACS, fluorescence-activated cell sorting.

any EI1 treatment (Figure 1c). As EZH2 and EZH1 are the only known mammalian H3K27 methyltransferases, we investigated if their expression had been altered in the resistant cells. No significant change of EZH2 and EZH1 expression was observed in K-R2 and K-R10 cells compared with K-P cells (Figure 1c).

To investigate whether PRC2 complexes were genetically altered in resistant cells, RNA-seq analysis was carried out. The EZH2 Y641N mutation showed an allele frequency of approximately 50% across all samples (K-P, K-R2 and K-R10), suggesting equal expression of EZH2 WT and Y641N. Importantly, two novel missense point mutations of EZH2 were identified in K-R2 and K-R10 (Figures 1a and d); these sequence alterations were also confirmed by Sanger sequencing (Supplementary Figure 1). A dinucleotide change of AT → TA resulted in a single amino-acid change at codon 111 from Tyrosine (Y) to Leucine (L) and a single-nucleotide change of T → A resulted in another amino-acid change at codon 661 from Tyrosine (Y) to Aspartic acid (D; Figure 1d). The allele frequency of Y111L was 32% and 47% in K-R2 and K-R10, respectively (Supplementary Table 1A), but not detected in K-P cells. The allele frequency of Y661D was 2% and 19% in K-R2 and K-R10, respectively, whereas only a very low level of this sequence alteration was detected in K-P cells (0.3%; Supplementary Table 1A). No sequence alterations were found in other PRC2 complex subunits including SUZ12, EED, AEBP2, RbAp48 and EZH1. K-R2- and K-R10-derived cell clones were sequenced by Sanger sequencing and the mutation spectra are shown in Figure 1a and Supplementary Table 1B. All clones contained the Y111L mutation. Although 3 out of 10 of K-R2-derived clones had the Y661D mutation, 9 out of 10 of K-R10-derived clones contained this mutation. Interestingly, Y661 is in close molecular proximity to the EZH2-activating mutation Y641N (Figure 1d) and the SAM/SAH (S-adenosylhomocysteine)-binding region (Figure 1e). Further analysis of the RNA-seq data showed that the Y661D mutation was always found in sequences where amino-acid residue 641 was N, therefore the Y661D mutation resided in the *EZH2*^{Y641N} allele. To investigate which *EZH2* alleles contained the Y111L alteration, mutant sequences were cloned from multiple clones and analyzed by Sanger sequencing. In contrast to Y661D, Y111L was only found in the context of the *EZH2*^{WT} allele. In summary, two secondary mutations of EZH2 were identified in the resistant cells: the Y111L mutation transforming the *EZH2*^{WT} allele and the Y661D mutation *cis* to the *EZH2*^{Y641N} allele. These data provide genetic evidence that both EZH2 WT and mutant proteins are targeted by EI1 in cells.

K-R2 and K-R10 cells were resistant to multiple EZH2 inhibitors

To evaluate if this mode of resistance was unique to EI1, we tested two additional EZH2 inhibitors, EPZ-6438[12] and compound 3[11] against four K-R2- and K-R10-derived cell clones. All three compounds inhibit EZH2 enzymatic activity through SAM-competitive mechanisms. However, EPZ-6438 and EI1 share the pyridone scaffold while compound 3 does not. EPZ-6438 was more effective compared with EI1 in reversing the cellular H3K27Me3 level to H3K27Me0 (Figure 2a) and was also more potent in inducing growth arrest (Figure 2b). Importantly, all four K-R2- and K-R10-derived cell clones were also refractory to EPZ-6438 in a cell proliferation assay, similar to EI1 (Figures 2c and d).

The 5-bromo-2-deoxyuridine (BrdU) incorporation assay is a more sensitive cellular assay to quantitate the anti-proliferative effect of EZH2 inhibitors. Cells were first treated with 10 μM EI1 or EPZ-6438 for 6 days and pulsed with BrdU at day 7 to quantitate actively proliferating cells undergoing DNA synthesis (Figure 2e). EI1 and EPZ-6438 almost completely suppressed DNA synthesis in K-P cells, causing >90% reduction of BrdU incorporation compared with the dimethyl sulfoxide (DMSO) control (Figure 2e). In all four resistant clones, EI1 treatment did not significantly inhibit BrdU incorporation compared with DMSO controls. With EPZ-6438, all four resistant clones showed partial resistance, as indicated by an intermediate reduction of BrdU incorporation compared with the DMSO-treated K-P control. The degree of resistance toward EPZ-6438 appeared more prominent in clones containing double EZH2 mutations, as KR-10#6 and #7 contain both Y111L and Y661D mutations, whereas the KR-2#4 and #5 only contain the Y111L mutation.

Compound 3 exhibited much weaker anti-proliferative activity, consistent with its weaker potency inhibiting the PRC2 complex *in vitro* (Table 2). Treatment of K-P cells with 10 μM of compound 3 for 6 days resulted in >60% reduction of BrdU incorporation compared with DMSO controls (Supplementary Figure 2). Noticeably, none of the resistant clones showed a decrease in BrdU incorporation compared with DMSO controls. Collectively, these data showed that the resistant cells were refractory to all EZH2 inhibitors tested.

PRC2$^{Y641N/Y661D}$ was refractory to biochemical inhibition by EZH2 inhibitors

Examination of the homology model of EZH2 shows that residue Y661D is in close proximity to the SAM/SAH-binding site (Figure 1e). The structural changes incurred by the Y661D mutation provide expanded volume in this region, increasing the distance between this residue and the centroid of any ligand occupying this pocket. The Y661 → D mutation would also change the hydrophilic nature of the binding site. Being a SAM-competitive inhibitor,[14] EI1 would likely occupy at least a portion of this binding site, and hence it is possible that the Y661D mutation might interfere with the binding of EI1 to EZH2.

To fully characterize their substrate specificity and inhibitor profile, WT and mutant PRC2 complexes were reconstituted *in vitro* (Supplementary Figure 3). Biochemical reactions were performed using H3 peptides (a.a. 21–44) with K27Me0, K27Me1 or K27Me2 as substrates. PRC2^{WT} was most active with H3K27Me0 and least active with H3K27Me2, whereas the PRC2^{Y641N} complex had the reverse substrate preference (Figure 3a and Table 1), consistent with a previous report.[9] PRC2$^{Y641N/Y661D}$ showed identical substrate preference as PRC2^{Y641N}, exhibiting undetectable activity with H3K27Me0 and increased activity with H3K27Me1 and Me2 (Figure 3a and Table 1). Steady-state kinetic analysis showed PRC2$^{Y641N/Y661D}$ had a higher K_m for SAM (5.1- and 3.8-fold for H3K27Me1 and Me2, respectively) compared with PRC2^{Y641N}. PRC2$^{Y641N/Y661D}$ also showed higher K_m for H3K27Me1 and Me2 (4- and 2.6-fold, respectively) compared with PRC2^{Y641N}. The catalytic efficiency (k_{cat}/K_m) of PRC2^{Y641N} was slightly higher compared with PRC2$^{Y641N/Y661D}$, with a noticeable threefold difference with H3K27Me1 (Table 1).

Next, we investigated if PRC2$^{Y641N/Y661D}$ can be inhibited by EZH2 inhibitors *in vitro*. Biochemical reactions were carried out with [SAM] at K_m value of 1 or 20 μM (approximating physiological concentrations). EI1, EPZ-6438 and compound 3 all showed much reduced potency to inhibit PRC2$^{Y641N/Y661D}$ compared with PRC2^{Y641N}. For example, when the reaction was carried out at 1 μM SAM, IC_{50} values of EI1 against PRC2$^{Y641N/Y661D}$ were >300-fold weaker compared with PRC2^{Y641N} with both H3K27Me1 and Me2 substrates (Supplementary Figure 4 and Supplementary Table 2). Importantly, EI1 showed IC_{50} values of 0.1 μM (H3K27Me1) and 0.2 μM (H3K27Me2) against PRC2^{Y641N} at 20 μM SAM, whereas it was inactive against PRC2$^{Y641N/Y661D}$ with an IC_{50} > 25 μM (for H3K27Me1 and Me2; Table 2 and Figure 3b). Similar results were observed with EPZ-6438 and compound 3 (Table 2, Supplementary Figures 5 and 6 and Supplementary Table 2). All three compounds also showed a shift in IC_{50} values when assayed at 1 μM versus 20 μM SAM, as expected for SAM-competitive inhibitors (Supplementary Figures 4–6). Taken together, the PRC2$^{Y641N/Y661D}$ complex was catalytically active and shared

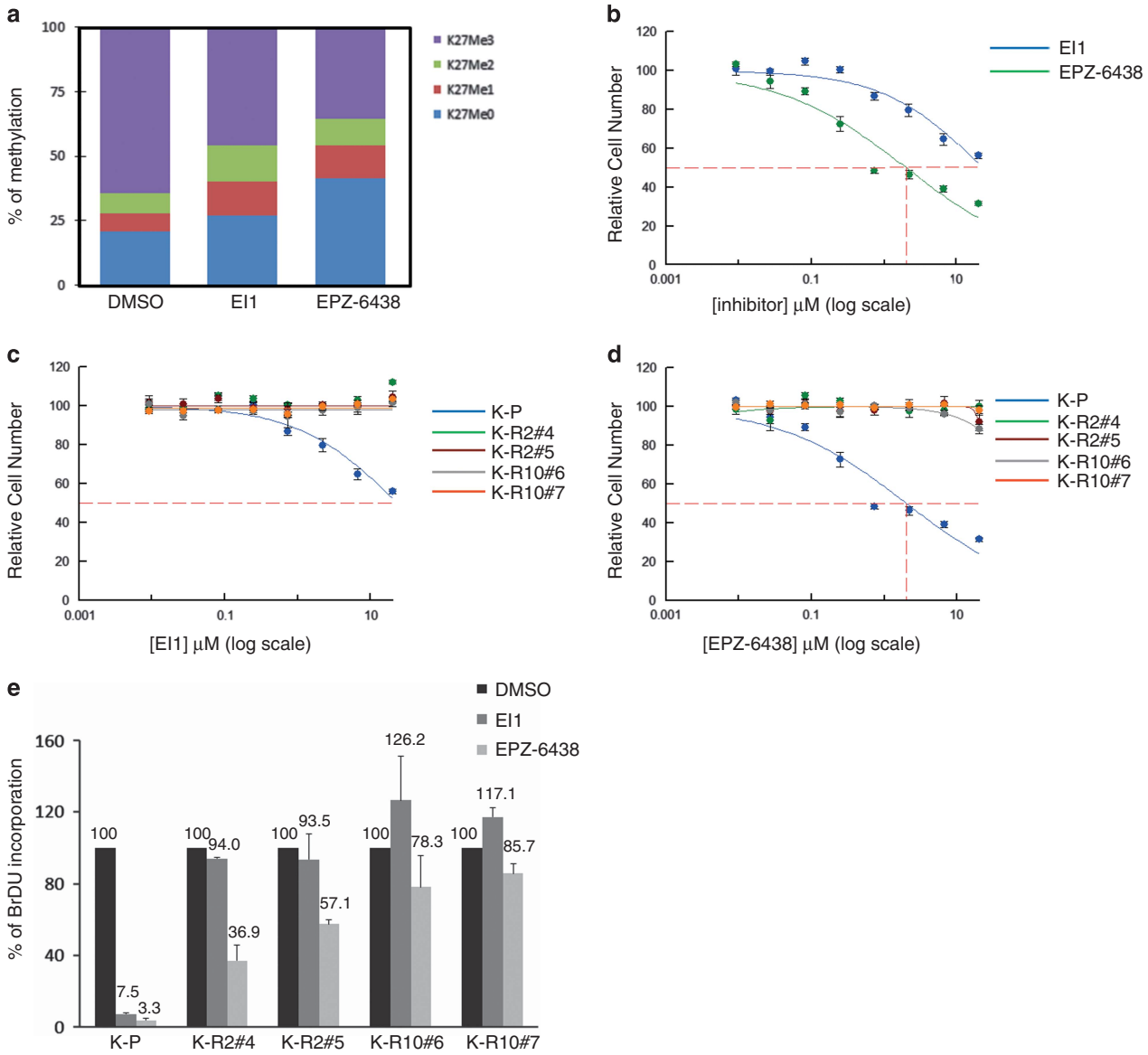

Figure 2. K-R2 and K-R10 cells showed resistance to multiple EZH2 inhibitors. (**a**) H3K27Me0, Me1, Me2, and Me3 were quantitated by mass spectrometry in K-P cells treated with 10 μM EI1 or EPZ-6438. (**b**) Growth inhibition by EI1 and EPZ-6438 in a 6-day proliferation assay. *Y*-axis shows percent of growth normalized to DMSO controls. (**c, d**) Growth inhibition by EI1 (**c**) and EPZ-6438 (**d**). (**e**) DMSO-treated samples are normalized to 100% BrdU incorporation (*Y*-axis) and percent of BrdU incorporation (average from two independent experiments) are indicated.

identical substrate preference with its predecessor PRC2^{Y641N} complex, but was refractory to biochemical inhibition by all EZH2 inhibitors.

Y111L mutation restored PRC2^{WT} activity in the presence of inhibitor to promote resistance

The Y111L mutation occurred in the context of the *EZH2^{WT}* allele and was present in all resistant clones. Seven out of the ten resistant clones derived from the 2 μM EI1 treatment group (KR-2) carried the Y111L mutation alone, suggesting this was sufficient to confer resistance to a low dose of EI1. We considered two different hypothetical mechanisms by which the Y111L mutation might confer resistance. First, Y111L might mimic Y641N function, exhibiting enhanced H3K27Me2 → Me3 activity to generate resistance. Alternatively, Y111L might maintain the biochemical properties of PRC2^{WT} but be refractory to inhibition by EZH2 inhibitors. The first scenario would imply that restoring the gain-of-function enzymatic activity is important for the development of resistance. If the latter is true, it would suggest restoration of EZH2 WT activity is a critical step toward resistance.

We carried out biochemical assays as above to characterize the PRC2^{Y111L} complex. Similar to PRC2^{WT}, PRC2^{Y111L} was active against H3K27Me0 and Me1 and was inactive against H3K27Me2 (Figure 3a and Table 1). k_{cat} and K_m values for SAM, H3K27Me0 and Me1 for PRC2^{Y111L} were similar to those of PRC2^{WT}, resulting in comparable catalytic efficiencies (k_{cat}/K_m) of the two complexes (Table 1). Next, experiments were carried out to evaluate the biochemical inhibition of PRC2^{WT} and PRC2^{Y111L} by EI1. When tested at 1 μM SAM, the IC_{50} of EI1 against PRC2^{111L} was 3.1 μM with H3K27Me0 and 4.2 μM with H3K27Me1, which were much weaker compared with those of PRC2^{WT} (0.02 and 0.009 μM for H3K27Me0 and Me1, respectively; Supplementary Figure 4 and

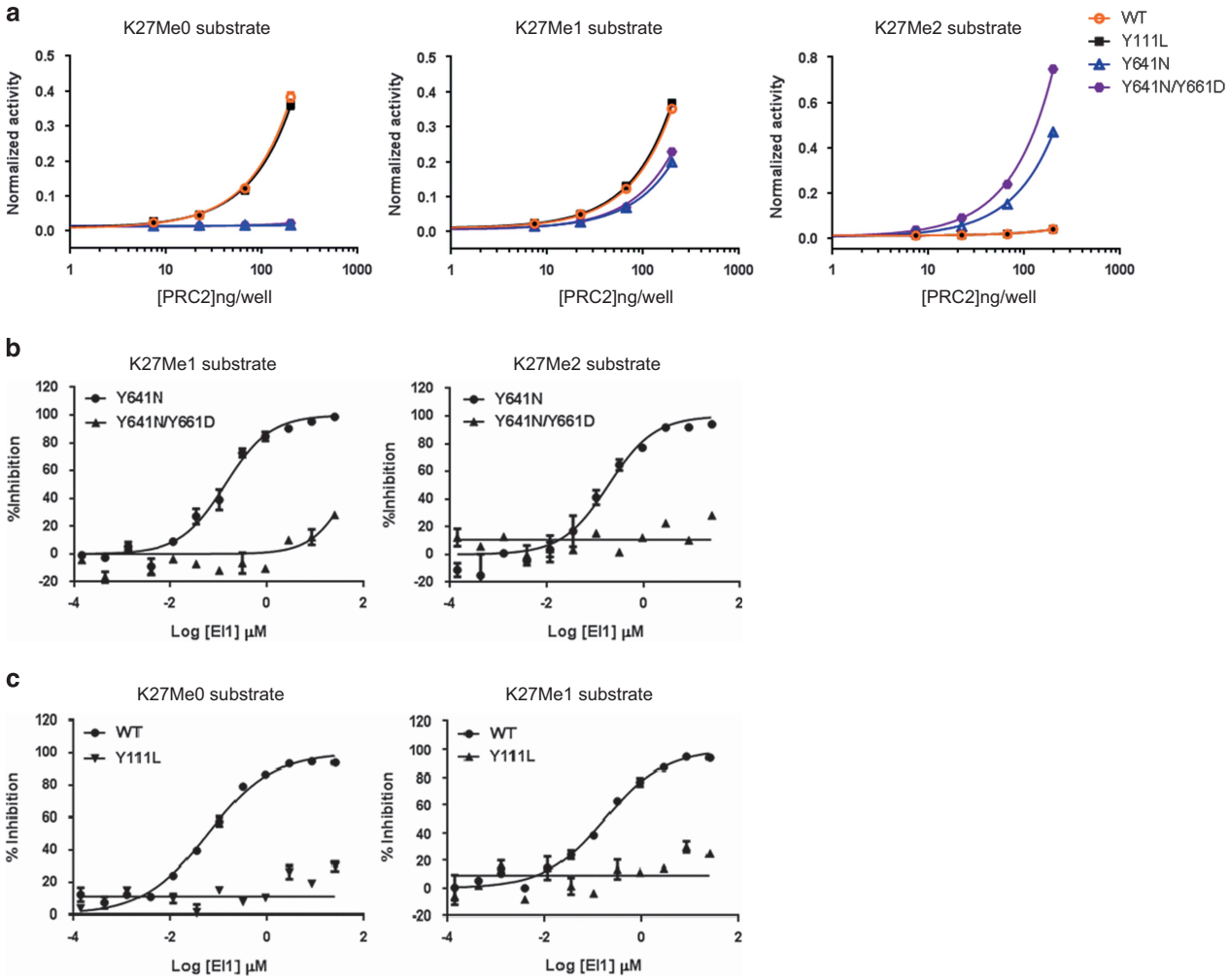

Figure 3. PRC2^{Y111L} and PRC2$^{Y641N/Y661D}$ were refractory to biochemical inhibition by EZH2 inhibitor. (**a**) Normalized activity of PRC2^{WT} (○), PRC2^{Y111L} (■), PRC2^{Y641N} (△) and PRC2$^{Y641N/Y661D}$ (⬣) at various enzyme concentrations with fixed [SAM] and three different H3 peptide substrates: H3K27Me0 (left), H3K27Me1 (middle) and H3K27Me2 (right). (**b**) Biochemical inhibition of PRC2$^{Y641N/Y661D}$ and (**c**) PRC2^{Y111L} by EI1. *Y*-axis indicates percent inhibition. Peptide substrates are listed, and [SAM] was 20 µM.

Table 1. Steady-state kinetic parameters for the methylation reaction catalyzed by PRC2^{WT}, PRC2^{Y111L}, PRC2^{Y641N} and PRC2$^{Y641N/Y661D}$

Proteins	*H3 peptide*	$K_{m,\ SAM}$ *(x10^{-6}M)*	$K_{m,\ H3\ (21-44)}$ *(x10^{-6}M)*	k_{cat} *(x10^{-2}/s)*	$k_{cat}/K_{m,\ H3\ (21-44)}$ *(x10^{4}/M/s)*
WT	21–44, Me0	1.1 ± 0.1	0.7 ± 0.08	1.6 ± 0.05	2.4 ± 0.1
	21–44 [K27-CH_3], Me1	1.3 ± 0.2	0.9 ± 0.1	1.7 ± 0.06	1.9 ± 0.1
	21–44 [K27-CH_3]$_2$, Me2	–	–	–	–
Y111L	21–44, Me0	0.9 ± 0.1	0.9 ± 0.1	1.6 ± 0.05	1.8 ± 0.1
	21–44 [K27-CH_3], Me1	1.5 ± 0.2	1.4 ± 0.2	1.9 ± 0.1	1.4 ± 0.1
	21–44 [K27-CH_3]$_2$, Me2	–	–	–	–
Y641N	21–44, Me0	–	–	–	–
	21–44 [K27-CH_3], Me1	0.9 ± 0.1	0.7 ± 0.09	0.6 ± 0.02	0.9 ± 0.1
	21–44 [K27-CH_3]$_2$, Me2	1.2 ± 0.1	1.1 ± 0.10	2.4 ± 0.06	2.2 ± 0.09
Y641N/Y661D	21–44, Me0	–	–	–	–
	21–44 [K27-CH_3], Me1	4.6 ± 1.0	2.8 ± 0.6	0.9 ± 0.07	0.3 ± 0.2
	21–44 [K27-CH_3]$_2$, Me2	4.5 ± 0.3	2.9 ± 0.2	4.4 ± 0.1	1.5 ± 0.06

Abbreviations: WT, wild type; '-', not determined.

Supplementary Table 2). The IC_{50} of EI1 for PRC2^{WT} was 0.2 µM and 0.06 µM with Me0 and Me1 substrate, respectively, at 20 µM SAM (Table 2), but EI1 was inactive against PRC2^{Y111L} (Figure 3c). Similar results were also observed with EPZ-6438 and compound 3 (Table 2, Supplementary Figures 5 and 6 and Supplementary Table 2). Therefore, PRC2^{Y111L} retained the same substrate specificity as PRC2^{WT} but became refractory to biochemical inhibition by EZH2 inhibitors. These results suggested that restoring EZH2 WT activity is important for resistance and tumor growth and proliferation.

We further tested whether Y111L and Y661D mutations might affect EI1 binding to PRC2 complexes by using differential scanning fluorimetry. When EI1 was incubated with PRC2^{WT} or PRC2^{Y641N},

Table 2. IC50 values for EI1, EPZ-6438 and compound 3 against $PRC2^{WT}$, $PRC2^{Y111L}$, $PRC2^{Y641N}$ and $PRC2^{Y641N/Y661D}$

Inhibitor	*Substrate*	*WT (μM)*	*Y111L (μM)*	*Y641N (μM)*	*Y641N/Y6661D (μM)*
EI1	Me0	0.2 ± 0.03	> 25	(−)	(−)
	Me1	0.06 ± 0.0	> 25	0.1 ± 0.03	> 25
	Me2	(−)	(−)	0.2 ± 0.05	> 25
EPZ-6438	Me0	0.2 ± 0.04	11.5 ± 4.3	(−)	(−)
	Me1	0.06 ± 0.01	9.2 ± 2.7	0.1 ± 0.03	2.8 ± 1.1
	Me2	(−)	(−)	0.1 ± 0.04	3.4 ± 0.8
Compound 3	Me0	2.02 ± 0.4	> 25	(−)	(−)
	Me1	0.9 ± 0.2	> 25	6.1 ± 0.8	> 25
	Me2	(−)	(−)	8.7 ± 1.1	> 25

Abbreviation: WT, wild type. The biochemical reaction was carried out with [SAM] at 20 μM. The assay was carried out with [SAM] of 20 μM. When indicated with (-), those conditions were not tested due to low basal activity.

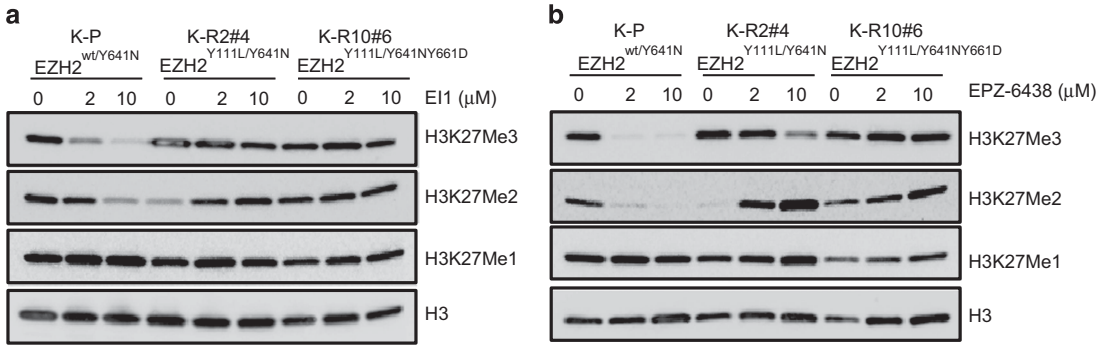

Figure 4. Restoration of cellular H3K27Me3 correlated with resistance to EZH2 inhibitors. Western blot of H3K27Me3, Me2 and Me1 in the indicated samples treated with EI (**a**) or EPZ-6438 (**b**). Histone H3 was used as the loading control.

we observed a T_m shift of 4.6 and 2.3°C, respectively, which was indicative of compound interaction with the PRC2 complexes (Supplementary Table 3). No significant T_m shifts were observed when the experiment was performed using $PRC2^{Y111L}$ or $PRC2^{Y641N/Y661D}$. These results are consistent with the hypothesis that the resistant mutations interfere with EI1 binding to PRC2 complexes.

Restoration of cellular H3K27Me3 correlated with resistance to EZH2 inhibitors

Western blot analysis and histone tail profiling were carried out to evaluate H3K27 methylation states in sensitive and resistant cells. As K-P cells express both EZH2 WT and Y641 mutant proteins, it was hypothesized that H3K27Me1 and Me2 produced by EZH2 WT would then be methylated by EZH2 Y641N to generate elevated levels of H3K27Me3, thereby promoting tumorigenesis.[9] When K-P cells were treated with increasing doses of EI1, both H3K27Me2 and Me3 levels decreased (Figure 4a), consistent with previous reports.[13–15] Histone tail profiling by mass spectrometry provided further resolution of different methylated H3 peptides (Supplementary Figure 8). Similar to the western blot analysis, K27Me3 methylated peptides showed the greatest decrease following treatment with EI1 (> 2-fold), whereas multiple K27Me0 and Me1 peptides were increased, suggesting accumulation in K27Me0 and Me1 states (Supplementary Figure 8). Unlike K-P cells, the presence of Y111L and Y661D mutations in K-R10 clones suppressed the effect of EI1 on H3K27Me2 or Me3 inhibition (Figure 4a, compare lanes 8 and 9 to lane 7), agreeing with the biochemical observations that $PRC2^{Y111L}$ and $PRC2^{Y641N/Y661D}$ were refractory to EI1. Histone profiling also showed that EI1 caused minimal decrease of H3K27Me3 peptides in K-R10 clones compared with K-P cells (Supplementary Figure 8). Interestingly, the presence of the Y111L mutation alone in K-R2 clones was able to significantly limit the extent of H3K27Me3 inhibition by EI1 when compared with K-P cells (Figure 4a, compare lanes 5 and 6 to lane 4 and lanes 2 and 3 to lane 1). Histone profiling also showed that production of different H3K27Me3 peptides was inhibited much less by EI1 compared with K-P cells (Supplementary Figure 8). Importantly, unlike K-P cells that showed accumulation of K27Me0 and Me1 states, H3K27Me2 peptides showed the most pronounced accumulation in K-R2 clones (Figure 4a and Supplementary Figure 8). As the Y111L mutation rescued K27Me0 → Me1 and Me2 conversion in the presence of inhibitor, the accumulation in H3K27Me2 intermediates now reflects the inhibition of the Y641N mutant protein in K-R2 clones. The experiments with EI1 were also repeated with EPZ-6438 and additional cell clones (Figure 4b and Supplementary Figures 7A and 8). We noticed that K-R2#4 cells showed a reduced basal level of H3K27Me2 and an increased level of H3K27Me3 compared with K-P cells in western blot analysis (Figures 4a and b, compare lane 4 to lane 1). $PRC2^{Y111L}$ exhibited slightly reduced catalytic efficiency for both H3K27Me0 and Me1 substrates when compared with $PRC2^{WT}$ (Table 1), which could explain this difference. Western blot analysis and histone profiling also showed that the effects of EI1 and EPZ-6438 were very specific toward H3K27 methylation; no noticeable decrease in H3K4, K9, K36 and K79 methylation was observed (Supplementary Figures 7B and C).

In summary, these data suggest that different H3K27 methylation states in EZH2 mutant lymphoma cells are highly influenced by the level of EZH2 WT enzymatic activity. When EZH2 WT activity (and the conversion of Me0 to Me1/2) is restored, it greatly limits the ability of EZH2 inhibitors to suppress H3K27Me3. Although the Y641N mutant protein is typically subject to inhibition by these

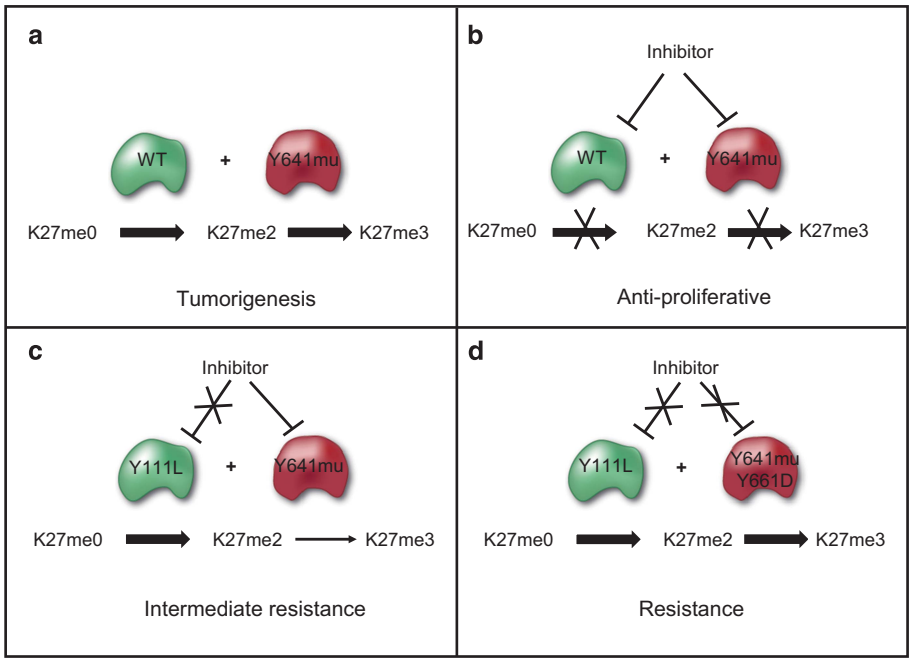

Figure 5. A model of resistance mechanism. (**a**) EZH2 WT and Y641N cooperate in cells to promote a hyper-activated state of H3K27Me3 and tumorigenesis. EZH2 WT has a critical priming role in generating H3K27Me1 and Me2, which serve as substrates for Y641N to produce H3K27Me3 product. (**b**) EZH2 inhibitors targeted both EZH2 WT and Y641N to inhibit H3K27Me3 and H3K27Me2 production and tumor cell growth. (**c**) An intermediate resistant state where EZH2 WT activity (K27me0 → me1/me2) was restored by the Y111L mutation, which also partially rescued the H3K27Me3 level and tumor cell growth. (**d**) Complete resistance was achieved when both *EZH2* alleles were mutated and became refractory to inhibitor.

agents, in the context of Y111L, this inhibition is to a significant extent abrogated. Although it was postulated that PRC2 WT and mutant complexes cooperate to promote a hyper-activated state of H3K27Me3 and tumorigenesis, these results provide the first evidence that targeting the EZH2 WT enzyme contributes most to the decrease of K27Me3 levels, and likely also contributed significantly to the anti-tumor effect.

DISCUSSION

EZH2 is required to maintain the tumorigenic phenotype, which has provided a strong rationale to develop an EZH2 inhibitor for cancer treatment.[5,20] With EZH2 inhibitors in the clinic, it is important to understand if targeted epigenetic therapeutics such as EZH2 inhibitors will have an effective and durable anti-cancer response.

In this study, we identified two novel EZH2 mutations (Y111L and Y661D) that were sufficient to confer resistance to EZH2 inhibitors in a KARPAS422 lymphoma cell model. Both PRC2^{Y111L} and PRC2$^{Y641N/Y661D}$ complexes were enzymatically active and retained substrate specificity identical to their predecessor complexes, but were refractory to inhibition by three different EZH2 inhibitors tested. Y661 resides within the SET domain in close proximity to the SAM-binding site. Conceivably, this mutation might directly impact inhibitor binding to EZH2. Y111 does not reside in any characterized functional domains and it is unknown if it will interact with SAM binding. The SAM-binding pocket was found to be absent in one study examining the X-ray crystallographic structure of the EZH2 SET domain,[21] which can explain why EZH2 alone lacks enzymatic activity. A minimal PRC2 complex consisting of EZH2, EED and SUZ12 is required for methyltransferase activity and the EZH2 SET domain is predicted to undergo conformational change upon complex formation, thus promoting SAM binding. Future efforts to obtain PRC2 complex-EI1 inhibitor co-crystal structures will enable mechanistic understanding of how Y111L and Y661D mutations affect EI1 binding to PRC2.

It has been postulated that EZH2 WT cooperates with the Y641 mutant form to promote H3K27Me3 and tumorigenesis.[9] Our data suggest that cooperation between EZH2 WT and the mutant is also important in the development of drug resistance. In this model, EZH2 WT carries out an important priming step to generate K27Me1 and Me2 substrates, which are then further methylated by the Y641N enzyme to form H3K27Me3, driving tumorigenesis (Figure 5a). EZH2 inhibitors affect both EZH2 WT and Y641N mutants to generate decreased levels of H3K27Me3 and H3K27Me2 and result in inhibition of cancer cell growth (Figure 5b). When the *EZH2 WT* allele was mutated to become refractory to inhibitor, the priming step was restored and, remarkably, this change was able to limit the consequent impact on cellular H3K27Me3, enabling a partial resistance state (Figure 5c). Complete resistance was achieved with a second mutation to the *EZH2*^{Y641N} allele, and thus both EZH2 proteins (EZH2^{Y111L} and EZH2$^{Y641N/Y661D}$) became refractory to inhibitors (Figure 5d). As resistant cells were only recovered from the initial 2 μM, but not the initial 10 μM, EI1 treatment group, we hypothesized that when cells were exposed to a higher dose of EZH2 inhibitor beyond a threshold level, cancer cells would need to acquire at least two simultaneous mutations (to both *EZH2*^{WT} and *EZH2*^{Y641N} alleles) to develop resistance. This possibility should be further investigated in the clinic to manage the potential emergence of resistance. Our model also suggests that EZH2 WT has a critical priming role to promote and maintain a high K27Me3 state in cells, so that targeting EZH2 WT activity might contribute to most of the anti-tumor effect produced by EZH2 inhibitors. Given that both EZH1 and EZH2 can generate K27Me1 and Me2,[3,9] more comprehensive studies are needed to address if EZH1 might also contribute to this resistance.

EZH2 inhibitors were shown to have impressive anti-tumor effects in tumor xenograft studies[12,13,16] and two studies showed that high-dose EPZ-6438 treatment caused complete tumor regression without tumor regrowth even after cessation of the dosing.[12,16] Interestingly, tumor regrowth was observed when a

lower dose of EPZ-6438 was used, one which initially induced tumor stasis. Furthermore, high-dose EPZ-6438 induced partial tumor regression in the WSU-DLCL2 xenograft model, which seems to become refractory to inhibitor treatment at the end of the 28-day treatment cycle.[12] It will be important to perform additional *in vivo* experiments to more comprehensively characterize resistance to EZH2 inhibitors *in vivo*.

Using *in vitro* models to predict resistance mechanisms has helped the drug discovery and development effort by allowing advance formulation of strategies to treat resistance. For example, BRAF mutant melanoma can develop resistance to allosteric MEK inhibitors, and random mutagenesis studies using an *in vitro* model successfully predicted a number of MEK1 mutations, which were subsequently validated in clinic.[22] Clinically relevant mutations of BCR-ABL against Imatinib were faithfully recaptured using cell line models,[23] which necessitated the development of novel BCR-ABL inhibitors to bypass Imatinib resistance.[24] Our study demonstrated that on-target mutations of EZH2 can occur to create resistance to EZH2 inhibitors. These results have at least two important implications for drug development and the clinical translation of EZH2 inhibitors. First, monitoring secondary mutations of EZH2 in clinical settings of primary and acquired resistance to treatment will be warranted. Second, development of novel EZH2 inhibitors against potential resistance mutations should be investigated in advance. As the current EZH2 inhibitors all act through a SAM-competitive mechanism to inhibit EZH2, and the resistant mutations showed cross-resistance to all SAM-competitive inhibitors, SAM non-competitive inhibitors might be exploited to bypass resistance. SAM non-competitive inhibitors have been reported for histone methyltransferases such as G9a and SYMD2.[25,26] These inhibitors affected the binding of histone peptide substrates to inhibit the enzymatic activity. Recently, Kim *et al* [27] also reported an EZH2-EED stapled peptide that disrupted the PRC2 complex and inhibited its enzymatic activity. By combining different types of EZH2 inhibitors, it might be possible to achieve a more durable and effective anti-tumor response by preventing the development of resistance.

MATERIALS AND METHODS

Cell culture, cell growth assay and western blot

Karpas422 cells were cultured in RPMI-1640 (Invitrogen, Grand Island, NY, USA; cat.#11875) with 10% FBS (Hyclone, Logan, UT, USA; cat. #SH30071.03) in a humidified incubator at 37 °C with 5% CO_2. K-R2 and K-R10 cells were cultured in growth media supplemented with 2 and 10 μM EI1, respectively. Single clones were isolated using an ARIA II cell sorter (BD Biosciences, Franklin Lakes, NJ, USA). Viable cell number was determined by Vi-CELL (Beckman Coulter, Indianapolis, IN, USA). Cell number was recorded and calculated with a splitting ratio to adjust for total cell numbers. Details of the cellular assays and antibody information are described in the Supplementary Information.

RNA-seq and TA cloning

RNA was purified using the RNeasy Mini RNA extraction kit (Qiagen, Valencia, CA, USA; cat. #74106). The protocol for RNA-seq analysis was previously described.[28] cDNA was synthesized using IScript (Bio-Rad, Hercules, CA, USA; cat. #170-8891). PCR was carried out using Phusion High Fidelity PCR master mix (Thermo, Waltham, MA, USA; cat. #F531L) and primers EZH2-F: 5′-GGGCCAGACTGGGAAGAAAT-3′ and EZH2-R: 5′-ACA CTTTGCAGCTGGTGAGA-3′. Amplicons were purified using the QIAquick PCR purification kit (Qiagen; cat. #28104). TA cloning was performed using TOPO TA cloning kit (Invitrogen; cat. #45-0030).

Histone profiling by mass spectrometry

Histones were extracted from cell pellets (5×10^6 cells) using a Histone Purification Kit (Active Motif, Carslbad, CA, USA; cat. #40026). The enriched histones were derivatized to block free lysines and analyzed by high-resolution mass spectrometry to assess histone methylation. See reference for a detailed protocol.[29]

Biochemical assays

PRC2 complexes were generated and purified using the baculovirus system as previously described.[14,30] The liquid chromatography-mass spectrometry assay detecting SAH was performed as previously described.[14,30] Details of the biochemical assays is described in the Supplementary Information.

Inhibitors were tested in a 12-point, threefold dose–response methyltransferase assay. For WT and Y111L enzymes, unmethylated and monomethylated histone peptide substrates were used. For Y641N and Y641N/Y661D mutants, monomethylated and dimethylated histone peptide substrates were used. 30 μM peptide substrates were used and SAM was present at 1 μM or 20 μM. 16 nM of each enzyme was used and reaction was carried out for 1 h. Percent inhibitions were calculated and plotted against logarithmic concentration of inhibitors, and data were fitted in the following model using GraphPad Prism v6.02.

$$Y = 100/(1 + 10\hat{}((\mathrm{LogIC}_{50} - X) * \mathrm{HillSlope})) \quad (1)$$

Y = %inhibition and X = log [inhibitor].

Differential scanning fluorimetry

PRC2 complexes (1 mM), SYPRO-orange (5×; Invitrogen; cat. #S6650), and Reaction Buffer (1X Tris-Buffered Saline, pH 8.0, 0.25 mM TCEP, ± 100 μM SAM) were incubated in the presence or absence of 100 μM EI1 with a temperature ramp from 25 to 85 °C with a 0.5 °C increment every 30 s. Fluorescence intensity was monitored using the Stratagene Mx3005P thermocycler (Agilent Technologies). The thermal transition (T_m) corresponds to the inflection point of the transition curve (fluorescence unit = $f(T)$) and was calculated as the maximum of the first derivative. All reactions were performed in triplicate.

Structural modeling

To examine the structure-function impact of the mutated residues, a homology model of the EZH2 SET domain was derived from the published crystal structure of the SET domain of GLP (EHMT1, PDB: 3HNA, resolution 1.5 A).[31] Y641 and Y661D mutations were then manually introduced into the EZH2 structure model and locally minimized with Molsoft ICM. The final all-atom RMSD (root-mean-square deviation; original GLP to mutant EZH2) was < 0.8 Å.

CONFLICT OF INTEREST

The authors declare no conflict of interest.

ACKNOWLEDGEMENTS

We acknowledge members of the oncology research and Novartis Institute of Biomedical Research (Shanghai, China), particularly the group involved in EZH2 program. We thank Drs A Wylie, S Sharma, PD Fortin, DR Kipp, G Leung, K Hurov, W Shao and W Sellers for helpful discussions, proof-reading the manuscript and sharing of reagents. All authors were employees of Novartis when the work was carried out.

REFERENCES

1 Boyer LA, Plath K, Zeitlinger J, Brambrink T, Medeiros LA, Lee TI *et al.* Polycomb complexes repress developmental regulators in murine embryonic stem cells. *Nature* 2006; **441**: 349–353.
2 Lee TI, Jenner RG, Boyer LA, Guenther MG, Levine SS, Kumar RM *et al.* Control of developmental regulators by Polycomb in human embryonic stem cells. *Cell* 2006; **125**: 301–313.
3 Shen X, Liu Y, Hsu YJ, Fujiwara Y, Kim J, Mao X *et al.* EZH1 mediates methylation on histone H3 lysine 27 and complements EZH2 in maintaining stem cell identity and executing pluripotency. *Mol Cell* 2008; **32**: 491–502.
4 Margueron R, Reinberg D. The Polycomb complex PRC2 and its mark in life. *Nature* 2011; **469**: 343–349.
5 Chase A, Cross NC. Aberrations of EZH2 in cancer. *Clin Cancer Res* 2011; **17**: 2613–2618.
6 Simon JA, Lange CA. Roles of the EZH2 histone methyltransferase in cancer epigenetics. *Mutat Res* 2008; **647**: 21–29.
7 Morin RD, Johnson NA, Severson TM, Mungall AJ, An J, Goya R *et al.* Somatic mutations altering EZH2 (Tyr641) in follicular and diffuse large B-cell lymphomas of germinal-center origin. *Nat Genet* 2010; **42**: 181–185.

8 Jaffe JD, Wang Y, Chan HM, Zhang J, Huether R, Kryukov GV *et al.* Global chromatin profiling reveals NSD2 mutations in pediatric acute lymphoblastic leukemia. *Nat Genet* 2013; **45**: 1386–1391.
9 Sneeringer CJ, Scott MP, Kuntz KW, Knutson SK, Pollock RM, Richon VM *et al.* Coordinated activities of wild-type plus mutant EZH2 drive tumor-associated hypertrimethylation of lysine 27 on histone H3 (H3K27) in human B-cell lymphomas. *Proc Natl Acad Sci USA* 2010; **107**: 20980–20985.
10 Yap DB, Chu J, Berg T, Schapira M, Cheng SW, Moradian A *et al.* Somatic mutations at EZH2 Y641 act dominantly through a mechanism of selectively altered PRC2 catalytic activity, to increase H3K27 trimethylation. *Blood* 2011; **117**: 2451–2459.
11 Garapaty-Rao S, Nasveschuk C, Gagnon A, Chan EY, Sandy P, Busby J *et al.* Identification of EZH2 and EZH1 small molecule inhibitors with selective impact on diffuse large B cell lymphoma cell growth. *Chem Biol* 2013; **20**: 1329–1339.
12 Knutson SK, Kawano S, Minoshima Y, Warholic NM, Huang KC, Xiao Y *et al.* Selective inhibition of EZH2 by EPZ-6438 leads to potent antitumor activity in EZH2 mutant non-hodgkin lymphoma. *Mol Cancer Ther* 2014; **13**: 842–854.
13 McCabe MT, Ott HM, Ganji G, Korenchuk S, Thompson C, Van Aller GS *et al.* EZH2 inhibition as a therapeutic strategy for lymphoma with EZH2-activating mutations. *Nature* 2012; **492**: 108–112.
14 Qi W, Chan H, Teng L, Li L, Chuai S, Zhang R *et al.* Selective inhibition of Ezh2 by a small molecule inhibitor blocks tumor cells proliferation. *Proc Natl Acad Sci USA* 2012; **109**: 21360–21365.
15 Knutson SK, Wigle TJ, Warholic NM, Sneeringer CJ, Allain CJ, Klaus CR *et al.* A selective inhibitor of EZH2 blocks H3K27 methylation and kills mutant lymphoma cells. *Nat Chem Biol* 2012; **8**: 890–896.
16 Knutson SK, Warholic NM, Wigle TJ, Klaus CR, Allain CJ, Raimondi A *et al.* Durable tumor regression in genetically altered malignant rhabdoid tumors by inhibition of methyltransferase EZH2. *Proc Natl Acad Sci USA* 2013; **110**: 7922–7927.
17 Beguelin W, Popovic R, Teater M, Jiang Y, Bunting KL, Rosen M *et al.* EZH2 is required for germinal center formation and somatic EZH2 mutations promote lymphoid transformation. *Cancer Cell* 2013; **23**: 677–692.
18 Mack SC, Witt H, Piro RM, Gu L, Zuyderduyn S, Stutz AM *et al.* Epigenomic alterations define lethal CIMP-positive ependymomas of infancy. *Nature* 2014; **506**: 445–450.
19 Holohan C, Van SS, Longley DB, Johnston PG. Cancer drug resistance: an evolving paradigm. *Nat Rev Cancer* 2013; **13**: 714–726.
20 Helin K, Dhanak D. Chromatin proteins and modifications as drug targets. *Nature* 2013; **502**: 480–488.
21 Antonysamy S, Condon B, Druzina Z, Bonanno JB, Gheyi T, Zhang F *et al.* Structural context of disease-associated mutations and putative mechanism of autoinhibition revealed by X-ray crystallographic analysis of the EZH2-SET domain. *PLoS One* 2013; **8**: e84147.
22 Emery CM, Vijayendran KG, Zipser MC, Sawyer AM, Niu L, Kim JJ *et al.* MEK1 mutations confer resistance to MEK and B-RAF inhibition. *Proc Natl Acad Sci USA* 2009; **106**: 20411–20416.
23 Azam M, Latek RR, Daley GQ. Mechanisms of autoinhibition and STI-571/imatinib resistance revealed by mutagenesis of BCR-ABL. *Cell* 2003; **112**: 831–843.
24 Wehrle J, Pahl HL, von BN. Ponatinib: a third-generation inhibitor for the treatment of CML. *Recent Results Cancer Res* 2014; **201**: 99–107.
25 Ferguson AD, Larsen NA, Howard T, Pollard H, Green I, Grande C *et al.* Structural basis of substrate methylation and inhibition of SMYD2. *Structure* 2011; **19**: 1262–1273.
26 Vedadi M, Barsyte-Lovejoy D, Liu F, Rival-Gervier S, Allali-Hassani A, Labrie V *et al.* A chemical probe selectively inhibits G9a and GLP methyltransferase activity in cells. *Nat Chem Biol* 2011; **7**: 566–574.
27 Kim W, Bird GH, Neff T, Guo G, Kerenyi MA, Walensky LD *et al.* Targeted disruption of the EZH2-EED complex inhibits EZH2-dependent cancer. *Nat Chem Biol* 2013; **9**: 643–650.
28 Korpal M, Korn JM, Gao X, Rakiec DP, Ruddy DA, Doshi S *et al.* An F876L mutation in androgen receptor confers genetic and phenotypic resistance to MDV3100 (enzalutamide). *Cancer Discov* 2013; **3**: 1030–1043.
29 Hoffman GR, Rahal R, Buxton F, Xiang K, McAllister G, Frias E *et al.* Functional epigenetics approach identifies BRM/SMARCA2 as a critical synthetic lethal target in BRG1-deficient cancers. *Proc Natl Acad Sci USA* 2014; **111**: 3128–3133.
30 Kipp DR, Quinn CM, Fortin PD. Enzyme-dependent lysine deprotonation in EZH2 catalysis. *Biochemistry* 2013; **52**: 6866–6878.
31 Wu H, Min J, Lunin VV, Antoshenko T, Dombrovski L, Zeng H *et al.* Structural biology of human H3K9 methyltransferases. *PLoS One* 2010; **5**: e8570.

Supplementary Information accompanies this paper on the Oncogene website (http://www.nature.com/onc)